POTASSIUM CHANNEL KINETICS IN SQUID AXONS WITH ELEVATED LEVELS OF EXTERNAL POTASSIUM CONCENTRATION

JOHN R. CLAY

Intramural Research Program, National Institute of Neurological and Communicative Disorders and Stroke, Laboratory of Biophysics, National Institutes of Health at the Marine Biological Laboratory, Woods Hole, Massachusetts 02543

ABSTRACT Potassium ion current in squid axons is usually modified by the effects of ion accumulation in the periaxonal space during voltage-clamp depolarization. The time course of potassium channel activation and ion accumulation usually overlap. A widely accepted procedure for circumventing the effects of accumulation in measurements of activation kinetics consists of measuring the difference in the current at the end of a depolarizing pulse and immediately following return of the membrane potential to the holding level. This instantaneous jump procedure is based upon the assumptions that the potassium channel current-voltage relation (IV) is a linear function of the driving force, and that the IV and the potassium channel-gating kinetics are both independent of ion accumulation. The latter assumption appears to be appropriate for activation kinetics. However, both assumptions concerning the IV are incorrect, in general. Consequently, the jump procedure provides a misleading view of gating kinetics for membrane depolarizations that produce net current flow. Jump conductance measurements for depolarizations that produce little or no net current indicate that the Hodgkin-Huxley n^4 model of potassium channel kinetics is appropriate for the physiological range of membrane potentials.

INTRODUCTION

The time course of activation of potassium channel conductance in squid axons following membrane depolarization is usually modified by the effects of potassium ion accumulation in the periaxonal space between the axon membrane and the Schwann cell surrounding the axon. Accumulation reduces the driving force for potassium ion current with a time course that overlaps with the time course of channel activation. Consequently, membrane current measurements usually do not accurately reflect gating kinetics. Several authors have suggested that this problem can be circumvented by measuring the instantaneous change in membrane current following a jump in membrane potential to either the holding level or to a depolarized level different than that of the initial step (Hodgkin and Huxley, 1952*a*; Conti and Wanke, 1975; Fohlmeister and Adelman, 1982; Gilly and Armstrong, 1982). The rationale for this technique is the assumption that potassium ion current, I_K, can be described by $I_K(V, t) = g_K(V, t)\ (V - E_K)$, where V is the membrane potential, t is the time following initiation of membrane depolarization, and E_K is the potassium channel equilibrium potential. The current at the end of a voltage step is, therefore, given by $I_K(V_1, t) = g_K(V_1, t)\ (V_1 - E_K[t])$, where $E_K(t)$ denotes the effective equilibrium potential due to ion accumulation. The current immediately after stepping to a second potential, $V = V_2$, is described by a similar expression with V_1 replaced by V_2. The assumption that $g_K(V_1, t) = g_K(V_2, t)$ is usually made, since channel-gating kinetics do not appear to change instantaneously following a voltage jump. Similarly, the external ion concentration in the periaxonal space can be assumed to remain unchanged immediately following the change of membrane potential to V_2. Consequently, the difference between the current at the end of the first step and at the beginning of the second step can be used to give the conductance, i.e., $g_K(V_1, t) = (I_K[V_2, t] - I_K[V_1, t])/(V_2 - V_1)$. The effects of ion accumulation are removed by this procedure. However, this analysis is based on the additional assumptions that the instantaneous current-voltage relation (IV) is linearly dependent upon $(V - E_K)$, the slope of the IV is independent of external potassium ion concentration, K_o, and the activation of channels is also independent of K_o. The purpose of this report is to test these assumptions that underlie the jump conductance technique.

METHODS

The experiments in this report were performed on internally perfused squid giant axons using methods that have been previously described

(Clay and Schlesinger, 1982; 1983). The temperature for all experiments was 7°C. The internal constituents for all experiments were 300 mM K^+, 50 mM Fl^-, 25 mM HPO_4^{-2}, 200 mM glutamate, and 505 mM sucrose. The axons were superfused externally with artificial seawater (ASW) containing 0.5 μM tetrodotoxin, 10 mM Ca^{+2}, 50 mM Mg^{+2}, 1 mM Tris, 561 mM Cl^-, x mM K^+, and (440 − x) mM Na^+, where x = 50, 100, 200, 300. We also used ASW containing 500 mM K^+, 0 mM Na^+, 621 mM Cl^-, and all other constituents the same as in the 50, 100, 200, or 300 K ASW solutions. Liquid junction potentials were $\lesssim$3 mV. The results in Fig. 2 have been corrected accordingly. All other potentials represent nominal values.

RESULTS

Influence of K_o: Activation Kinetics and the IV Relation

The first part of this report concerns the assumptions that external potassium ions do not influence either the activation of potassium channels or the relative voltage dependence of the potassium channel current-voltage relation (IV). To test these assumptions, activation kinetics were measured from preparations in 50 and 500 K ASW with single depolarizing steps to −20, 0, . . . +120 mV. Results of this procedure from a single preparation are shown in Fig. 1. These results exhibit the familiar sigmoidal activation of channel conductance immediately following step depolarization, as well as a decrease in current due to ion accumulation or depletion several milliseconds thereafter. The current was inward for both −20 and 0 mV with 500 K_o because the potassium equilibrium potential, E_K, was 10 mV for this condition. The kinetics in 50 K ASW do not appear to be markedly different from those in 500 K ASW. A detailed comparison of these results requires the respective IV relations. These results were obtained from membrane depolarization lasting several milliseconds to either −40, −20, or 0 mV followed by a step of the membrane potential to −120, −100, . . ., +80 mV. Membrane current was measured 70 μs following the second step. This protocol permits determination of the relative effect of K_o on the IV in a single axon with minimal ion accumulation during the prepulse. Results of this procedure for an axon in 50 and 200 mM K ASW and a 7-ms depolarizing prepulse to 0 mV are shown in Fig. 2. Similar results for axons in 100 and 500 K_o are given in Clay and Shlesinger (1983). The IV is in general a nonlinear function of the driving force, and its slope at any given potential is modified by K_o. The theoretical curves in Fig. 2 are best fits to these experimental results of the Goldman-Hodgkin-Katz (GHK) theory (Goldman, 1943; Hodgkin and Katz, 1949). An effective K_o of 75 mM was used for the 50 K_o results to account for accumulation during the prepulse. Accumulation did not appear to be a factor in the 200 K_o results. The GHK model provides a sufficient description of the 200 K_o IV curve and it is also appropriate for K_o > 200 mM (Clay and Shlesinger, 1982). It deviates slightly from the experimental results for $0 \leq V \leq 80$ mV with $K_o \leq$ 100 mM, as demonstrated by the 50 K_o results in Fig. 2 and by the results for 100 K_o in Clay and Shlesinger (1983). However, it provides at least a fair approximation to these results as well. Consequently, the GHK equation was used to compare the kinetics in Fig. 1 for 50 and 500 K ASW. Specifically, the 500 K_o results were scaled by the factor

$$[K_{o,1} - K_i \exp(eV/kT]/[K_{o,2} - K_i \exp(eV/kT)], \quad (1)$$

where $K_{o,1}$ = 500 mM, $K_{o,2}$ = 50 mM, K_i = 300 mM, e is the unit electronic charge, k is the Boltzmann constant, T is the absolute temperature, and V is the membrane potential. Results of this procedure superimposed on the 50 K_o records are shown in Fig. 3 for V = 20, 40, . . . 120 mV. The rising phases of the scaled 500 K_o results overlap with the corresponding portions of the 50 K_o results. There is a slight difference in the kinetics near the peak of the response for $V \geq 60$ mV, which may reflect a difference in the accumulation time course in 50 K_o as compared with 500 K_o for these potentials. Nevertheless, the similarities of these results are more striking than are the differences.

The results in Fig. 3 provide the basis for the first major

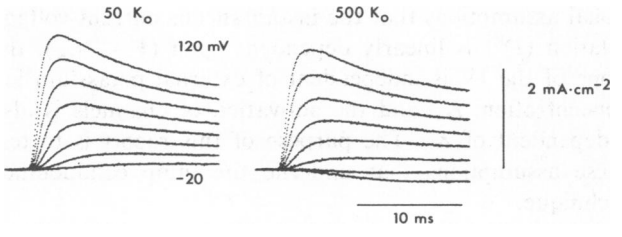

FIGURE 1 Superimposed records of potassium current from an axon in 50 and 500 K ASW in response to voltage-clamp steps to −20, 0, +20, . . . +120 mV from a holding potential of −80 mV. Corrections were made for capacitance and leakage currents. Axon C81.67.

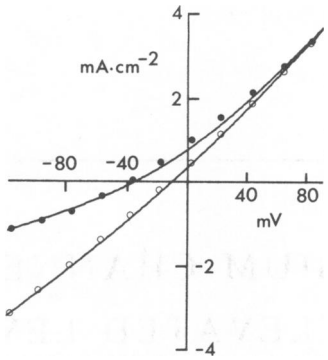

FIGURE 2 Current-voltage relations (IV) from an axon in 50 (●) and 200 (○) K ASW. The voltage-clamp protocol consisted of a 7-ms prepulse to 0 mV followed by a second step to −120, −100, −80, . . . +80 mV. The membrane current was measured 70 μs following the second step. Corrections were made for capacitance and leakage currents. The curves through the data points are best fits to these results of the Goldman-Hodgkin-Katz relation, which is given by $I_K = P_K \cdot F \cdot (eV/kT)\,(K_o - K_i \exp[eV/kT])/(1 - \exp[eV/kT])$, where F is the Faraday and P_K is the classically defined permeability coefficient. The best fit value of P_K was 0.33×10^{-4}cm · s^{-1} for both curves. The best fit values of K_o were 75 mM and 200 mM for the 50 and 200 K_o ASW results, respectively. Axon C80.11.

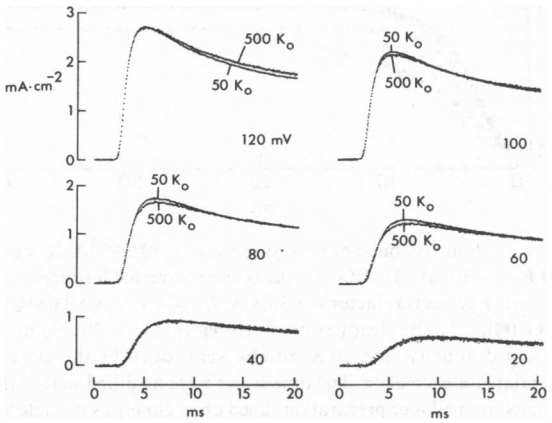

FIGURE 3 Direct comparison of the 50 and 500 K_o results in Fig. 1 for $V = +20, +40, \ldots +120$ mV. The 500 K_o results were corrected for 10% rundown of membrane current. These results were then scaled by the appropriate GHK factor, which is given by $(K_{o,1} - K_i \exp [eV/kT])/(K_{o,2} - K_i \exp [eV/kT])$ where $K_{o,1} = 500$ mM, $K_{o,2} = 50$ mM, and $K_i = 300$ mM. The scaled results are superimposed upon the corresponding 50 K_o records. (The scaling factor for the +20 mV 500 K_o record was 2.4 rather than the factor of 3.1 predicted by GHK).

conclusion of this paper, which is that activation kinetics in squid axons are not influenced by external potassium ions. Consequently, one of the assumptions underlying the jump conductance technique is appropriate. However, both of the assumptions concerning the IV relation are incorrect. The nonlinearity of the IV when $K_o \neq K_i$ and the influence of K_o on the slope of the IV are of critical significance in the analysis of the jump conductance measurements described below.

Jump Conductance Measurements

The results in this section are based on measurements of the potassium current at the end of a depolarizing pulse and at the beginning of the tail current following return of the membrane potential to the holding level. The current at the end of the depolarizing pulse is zero when the pulse potential is equal to E_K. The amplitude of the tail current for this condition provides a measure of channel activation during the depolarization. Consequently, channel-activation kinetics can be measured in the absence of ion accumulation with this technique by elevating K_o so that the pulse potential is equal to E_K. Results of this procedure from a single axon in 50, 100, 300, and 500 K_o with depolarizations to −40, −20, 0 and +20 mV, respectively, are shown in Fig. 4. The net current during the pulses was virtually zero in all cases, except for the 500 K_o results. The pulse potential in this case was slightly greater than E_K. The tail current kinetics, which are not the primary focus of this report, appear to be slowed somewhat by increases in K_o, which is consistent with the original observation of this effect by Swenson and Armstrong (1981). The tail current amplitudes for different levels of K_o cannot be directly compared because the current through an open channel at the holding potential, −80 mV, is a function of

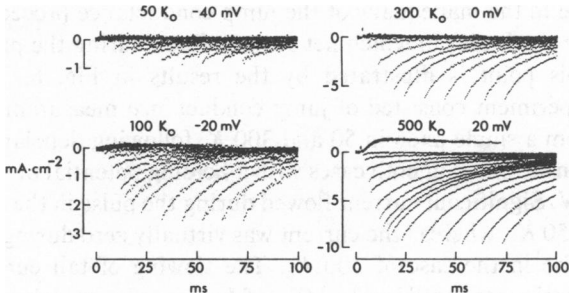

FIGURE 4 Superimposed records of tail currents from an axon in 50, 100, 300, and 500 K ASW and a prepulse to −40, −20, 0, and +20 mV, respectively, with prepulse durations as indicated, and a holding potential of −80 mV. Axon C81.03.

K_o. This effect was removed by scaling the results in Fig. 4 by the GHK factor given in Eq. 1. The results of this procedure are shown by the symbols (●) in Fig. 5. The channels were arbitrarily assumed to be fully activated in the steady state at $V = +20$ mV. The results for $V = -40$, −20, and 0 mV indicate the fraction of the conductance that is activated in the steady state at these potentials. The solid lines in Fig. 5 are best fits to these results of the original Hodgkin and Huxley (1952*b*) $n^4(t)$ model, where

$$n(t) = n_\infty + (n_o - n_\infty)e^{-t/\tau_n}, \qquad (2)$$

with $n_o = 0$. The best fit parameters, n_∞ and τ_n, are given for each set of measurements in Fig. 5. The n^4 model provides an adequate description for the activation kinetics. The slight deviation between the model and the 500 K_o results is

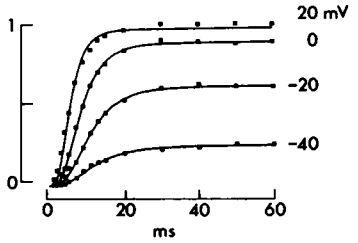

FIGURE 5 Relative amplitudes of jump kinetics from the records in Fig. 4. Each data point (●) corresponds to the difference between the current at the end of the pulse and 100 μs following return to the holding potential for the pulse potential and duration indicated. The 0 and +20 mV results were scaled for axon rundown by a factor of 1.7 and 1.9, respectively. The 20 mV (500 K_o) results were then scaled to unity from the average value of the 30, 40, 50, and 60 ms points. The −40, −20, and 0 mV points were scaled by the same factor. They were then scaled upward by the factor predicted by GHK. The latter scaling procedure was implemented by calculating the relative difference between the fully activated current at the prepulse level and the holding level from $V \cdot (K_o - K_i \exp [eV/kT])/(1 - \exp [eV/kT])$ with $K_i = 300$ mM and $K_o = 50$, 100, 300, or 500 mM. The 0 mV, 300 K_o results were scaled by the ratio of the GHK factor appropriate for $K_o = 500$ mM and the GHK factor appropriate for $K_o = 300$ mM. The −40 and −20 mV results were scaled in a similar manner. The solid lines (——) are best fits to these results of $n_\infty^4 (1 - \exp [-t/\tau_n])$ with $n_\infty^4 = 0.24$ and $\tau_n = 6.28$ ms for $V = -40$ mV; $n_\infty^4 = 0.61$ and $\tau_n = 5.67$ ms for $V = -20$ mV; $n_\infty^4 = 0.89$ and $\tau_n = 4.49$ ms for $V = 0$ mV; and $n_\infty^4 = 0.975$ and $\tau_n = 2.93$ ms for $V = +20$ mV.

due to the inadequacy of the jump conductance procedure for conditions in which net current flows during the pulse. This point is illustrated by the results in Fig. 6. This experiment consisted of jump conductance measurements from a single axon in 50 and 300 K_o following depolarizations to 0 mV in both cases with a holding potential of −80 mV. Significant current flowed during the pulse in the case of 50 K_o, whereas the current was virtually zero during the pulse in the case of 300 K_o. The slowing of tail current kinetics produced by elevation of K_o was pronounced in this preparation. The other significant aspect of these results is that the tail current amplitudes in 300 K_o reached a maximal value for depolarizations lasting 15–20 ms. The jump conductance measurement for 50 K_o reached a maximal value at later times. This result is further illustrated in Fig. 7, which consists of similar measurements from four axons in 50 and 300 K_o with pulses to 0 mV. The current and time axes were scaled so that these results from different preparations could be compared. The maximal tail current amplitudes in 300 K_o were scaled to unity for each axon. The 50 K_o results were also scaled by the same factor appropriate for each axon. The steady state measurements ($t > 20$ ms) in 50 and 300 K_o differ for reasons described below. The time coordinate for each axon was also scaled so that the 300 K_o results formed, as closely as possible, a smooth continuous curve. The 50 K_o results following the same time scaling procedure exhibited considerable scatter for $0 < t < 20$ ms. The solid line in Fig. 7 is the best fit to the 300 K_o results of the n^4 model. The dashed line represents the same curve with n_∞^4 adjusted ($n_\infty^4 = 0.85$) so that the line went through the 50 K_o points for $t > 20$ ms.

DISCUSSION

The results in Fig. 7 illustrate the primary finding of this report, which is that the jump conductance technique does not, in general, provide an accurate description of channel kinetics. If it did, the results in 50 and 300 K_o in Fig. 7 would overlap. The 50 K_o results describe a slow kinetic

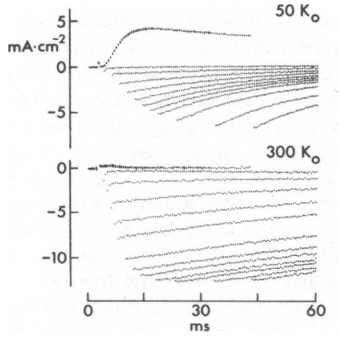

FIGURE 6 Superimposed records of membrane current in 50 and 300 K_o ASW for depolarizations of various durations to 0 mV followed by return of membrane potential to the holding level (−80 mV). The 300 K_o results were scaled by a factor of 1.75 to account for rundown of the potassium current. Axon C82.07.

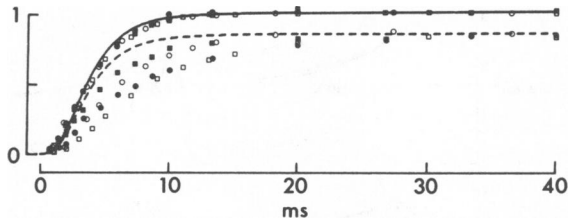

FIGURE 7 Jump conductance measurements in 50 and 300 K_o with V_1 = 0 and V_2 = −80 mV. The 300 K_o results were corrected for rundown: axon C82.06 (□), correction factor = 1.35; C82.07 (○), 1.75; C82.08 (●), 1.45; C82.11 (■), 1.1. The steady state measurements ($t \geq 20$ ms) in 300 K_o were scaled to unity. The 50 K_o results were scaled by the same factor appropriate for each axon. The time scales were modified so that the 300 K_o results from all four preparations lined up as closely as possible along a smooth curve. These time-scale factors were: C82.06, 1.0; C82.07, 1.1; C82.08, 1.5; C82.11, 1.5. The solid and (——) dashed lines (---) correspond to the n^4 model, as described in the text.

feature between 10 and 30 ms, which was not apparent in the 300 K_o results. This result is due to the effect of ion accumulation on the potassium channel IV during the pulse, as illustrated schematically in Fig. 8. The top part of Fig. 8 represents the effective IV relations for the experimental conditions of Figs. 6 and 7. During the first few milliseconds of the jump conductance measurements in 50 K_o, the IV relation is determined by the bulk external potassium ion concentration. The jump measurement (curve *b*, Fig. 8) directly corresponds to channel activation during the pulse. However, at later times the IV relation is determined by the effective ion concentration due to accumulation. After ~10–15 ms, the effective level of K_o is 100 mM. The steady state level ($t > 20$ ms) of K_o is ~200 mM. The IV curves for these conditions are shown in Fig. 8 at the appropriate times during the jump-measurement procedure. The IV changes shape so that the difference between the current at 0 mV, the pulse level, and −80 mV, the holding level, increases with time. This effect produces an apparent kinetic feature between 10 and 30 ms, as illustrated by curve *b* in Fig. 8. The IV relation for the bulk 300 K_o results remains unchanged throughout, because little or no current flows during the pulse. Consequently,

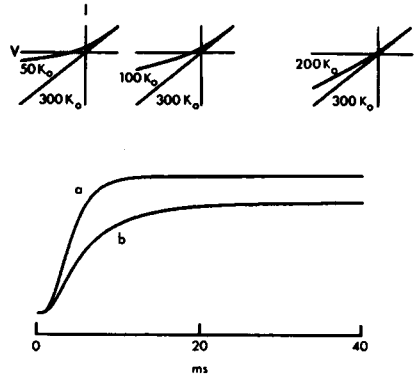

FIGURE 8 Schematic representation of the results in Fig. 7 as described in the text.

the time course of jump measurements in this case solely reflects channel activation (curve *a*, Fig. 8). The difference between the steady state levels of curves *a* and *b* in Fig. 8 is due to the fact that the final level of ion accumulation for the bulk 50 K_o results is ~200 mM. Consequently the difference between the current at 0 and −80 mV is less than it is for 300 K_o. The scatter in the experimental results in Fig. 7 for 50 K_o is due to variability in both the degree and the time course of accumulation for different preparations.

Several authors have used the jump conductance technique to determine potassium channel activation in squid axons. For example, Gilly, and Armstrong (1982) obtained results similar to the 50 K_o results in Fig. 7 with K_o = 100 mM, K_i = 275 mM, a pulse potential of +40 mV, and a holding potential of −70 mV. They attributed the relatively slow kinetic feature between 10 and 30 ms to a slow step in the channel-gating mechanism that is not contained in the original Hodgkin and Huxley (1952*b*) model (HH). Fohlmeister and Adelman (1982) also reported a slow kinetic feature based on a variation of the jump procedure. They measured the current both before and after the application of a small voltage step a few millivolts in amplitude at various times following a depolarizing pulse, which produced significant net outward current. This procedure circumvents the nonlinearity of the IV relation, but it does not circumvent the effect of accumulation on the slope of the IV.

The results in this report demonstrate that the original HH model is sufficient to describe the activation of potassium channels in squid axons in the physiological range of membrane potentials. The slight deviation between their n^4 model and the experimental results in Fig. 7 is approximately the same as the experimental error inherent in the jump procedure, especially for pulse depolarizations of brief duration. The HH model assumption of a linear IV relation is incorrect when the external K ion concentration is different than the internal K ion concentration. The results in this report and in Clay and Shlesinger (1983) demonstrate that the GHK model, rather than a linear relation, provides an approximate description of the experimental IV curve. This deficiency in the HH model can lead to an apparent discrepancy between the n^4 prediction and jump conductance measurements as this report has demonstrated. The slow kinetic feature between 10 and 30 ms in the results for 50 K_o in Fig. 7 is due to the effect of accumulation on the IV curve rather than to a slow step in channel gating. This result indicates that measurements of potassium channel kinetics in squid axons for depolarizations lasting several milliseconds, or longer, can only be made in the absence of ion accumulation.

The author gratefully acknowledges Ruthanne Mueller for technical assistance in these experiments and Dottie Leonard for cheerfully typing the manuscript.

Received for publication 13 January 1983 and in final form 3 June 1983.

REFERENCES

Clay, J. R., and M. F. Shlesinger. 1982. Delayed kinetics of squid axon potassium channels do not always superpose after time translation. *Biophys. J.* 37:677–680.

Clay, J. R., and M. F. Shlesinger. 1983. Effects of external cesium and rubidium on outward currents in squid giant axons. *Biophys. J.* 42:43–53.

Conti, F., and E. Wanke. 1975. Channel noise in nerve membranes and lipid bilayers. *Q. Rev. Biophys.* 8:451–506.

Fohlmeister, J. F., and W. J. Adelman, Jr. 1982. Anomalous potassium channel-gating rates as functions of calcium and potassium ion concentrations. *Biophys. J.* 37:427–431.

Gilly, W. F., and C. M. Armstrong. 1982. Divalent cations and the activation kinetics of potassium channels in squid giant axons. *J. Gen. Physiol.* 79:965–996.

Goldman, D. E. 1943. Potential, impedance, and rectification in membranes. *J. Gen. Physiol.* 27:37–60.

Hodgkin, A. L., and B. Katz. 1949. The effect of sodium ions on the electrical activity of the giant axon of the squid. *J. Physiol. (Lond.).* 108:37–77.

Hodgkin, A. L., and A. F. Huxley. 1952*a*. The components of membrane conductance in the giant axon of Loligo. *J. Physiol. (Lond.).* 116:473–496.

Hodgkin, A. L., and A. F. Huxley, 1952*b*. A quantitative description of membrane current and its application to conduction and excitation in nerve. *J. Physiol. (Lond.).* 117:500–544.

Swenson, R. P., Jr., and C. M. Armstrong. 1981. K^+ channels close more slowly in the presence of external K^+ and Rb^+. *Nature (Lond.).* 291:427–429.